ACTA CHEMICA SCANDINAVICA 14 (1960) 1161—1172

The Crystal Structure of Ti_5O_9

STEN ANDERSSON

Institute of Inorganic and Physical Chemistry, University of Stockholm, Stockholm, Sweden

The crystal structure of Ti_5O_9, the second member of the homologous series Ti_nO_{2n-1}, has been determined. It is triclinic, spacegroup $P\bar{1}$, with a cell content of 2 Ti_5O_9 and with unit cell dimensions $a = 5.569$ Å, $b = 7.120$ Å, $c = 8.865$ Å, $\alpha = 97.55°$, $\beta = 112.34°$ and $\gamma = 108.50°$. It may be described in terms of TiO_6-octahedra, which are joined by sharing edges and corners to form slabs of rutile structure, extending infinitely in two dimensions and possessing a finite width corresponding to five TiO_6 octahedra. The slabs are mutually connected by octahedra sharing faces.

The Ti_5O_9 structure provides the clue to the problem of finding the crystal structure of any member of the homologous series Ti_nO_{2n-1}, $Ti_{n-2}Cr_2O_{2n-1}$ and V_nO_{2n-1}.

The existence of a considerable number of discrete phases in the composition region $MO_{1.75-1.90}$ has been demonstrated for the titaniumoxygen system[1-3], for the titanium-chromium-oxygen system[4] and for the vanadium-oxygen systems[5]. The related and regularly changing appearance of the powder patterns of all these phases, the compositions of which are in close agreement with the general formula M_nO_{2n-1} (n integer), suggested that the various structures are all based on a common structural principle, in analogy with the case[6-8] for the molybdenum and the molybdenum wolfram oxides of the homologous series $(Mo,W)_nO_{3n-1}$.

It was thus thought possible to derive the structure of any member of the series M_nO_{2n-1} provided that the detailed structure of one homologue were known. This article gives an account of the structure determination of the phase Ti_5O_9. General structural data for the series will be given elsewhere[9].

EXPERIMENTAL

Details about the preparation and some other data concerning the $TiO_{1.80}$ sample have been given in previous communications[1,2]. Crystals of Ti_5O_9 were obtained by heating this sample at 1 150°C for three days in evacuated silica tubes. The crystals formed minute rods always found to be twinned. A fragment obtained by crushing a crystal was, however, found to have only a relatively small twin parasite, and was thus suitable for single-crystal studies.

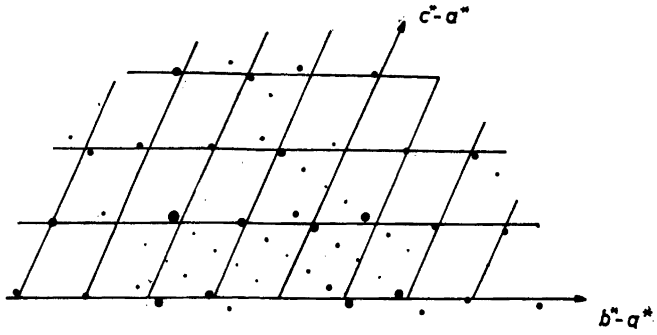

Fig. 1. The reciprocal lattice plane $h0l$ of Ti_5O_9. The networks represent the reciprocal lattice of the subcell (rutile).

Weissenberg photographs of the layer lines $(0-3, k, l)$ and $(h, 0-4, l)$ were registered with CuK radiation using multiple film techniques. The intensities of the reflexions were estimated visually.

A remarkable feature of the photographs was the extremely low number of reflexions hkl with k odd. Thus, the $(h1l)$ layer line contained only three strong, one medium and two weak reflexions.

Accurate unit cell dimensions were obtained from photographs taken in a Guinier focusing camera using strictly monochromatized Cu$K\alpha_1$ radiation and applying a procedure described in a previous communication from this Institute [10].

DERIVATION OF THE STRUCTURE

The single crystal data showed the structure to be triclinic, *i.e.* the symmetry should be $P1$ (No. 1) or $P\bar{1}$ (No. 2).

The Guinier powder photograph gave the following unit cell dimensions, referred to the lattice parameter of potassium chloride $a = 6.2919$ Å at 20 C:

$$a = 5.569 \text{ Å}, \quad b = 7.120 \text{ Å}, \quad c = 8.865 \text{ Å},$$
$$\alpha = 97.55°, \quad \beta = 112.34°, \quad \gamma = 108.50°.$$

The observed density of 4.29 indicated that the unit cell contains 2 formula units of Ti_5O_9, the calculated density being 4.31. The powder pattern has been published in a previous report [11].

The reciprocal lattice plane $h0l$, which is illustrated in Fig. 1, shows the presence of a pronounced substructure in real space. By considering the three-dimensional data, it was found that the substructure unit coincides with the structure of the rutile type, as was already suggested by the appearance of the powder pattern [1-3]. The [010]-direction of Ti_5O_9 was found to correspond to [111] of rutile. The structure determination could thus be started along the lines developed by Magnéli [7,8,12,13] when studying several molybdenum and wolfram oxides and especially $W_{20}O_{58}$.

The substructure character in this case implies that the strong reflexions of Ti_5O_9 occur close to the reciprocal lattice points of rutile. Assuming the structure to possess a centre of symmetry, the various strong reflexions were

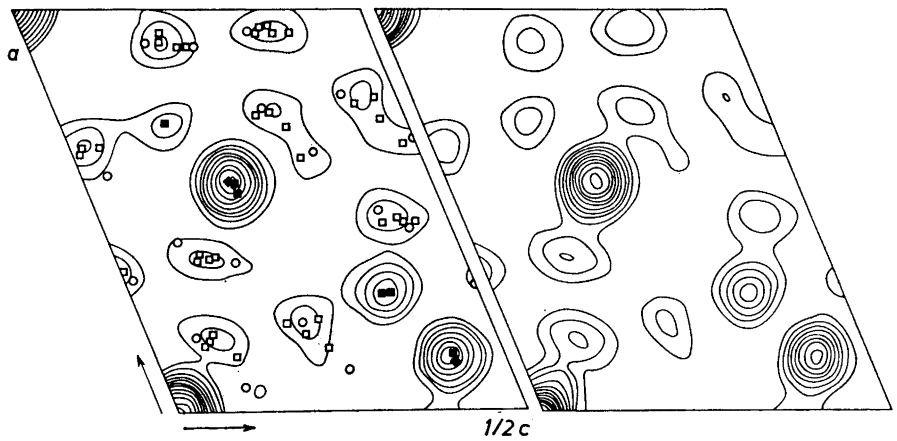

Fig. 2. Patterson projections along [010]. 1) Calculated from $|F|^2_{obs}$. 2) Calculated from $|F|^2_{calc}$. ◆ : Ti-Ti vectors (Multiplicity 8); ■ : Ti-Ti vectors (Multiplicity 4); □ : Ti-O vectors (Multiplicity 4); O : Ti-O vectors (Multiplicity 2).

assigned the signs of the corresponding rutile reflexions. This was done for two alternatives, *viz.* with a metal atom in or not in the origin position.

The two-dimensional Fourier sum* calculated over the strong reflexions *h0l*, which should correspond to a projection parallel to [010] of the "electron density function" for both alternatives, showed heavy maxima which could be attributed to titanium atoms and also minor ones which might be interpreted as due to oxygen atoms. Both alternatives were in fair agreement with the Patterson projection along [010] illustrated in Fig. 2 : 1. By including more reflexions in the Fourier sum, it was found possible to arrive at an index of agreement

$$\frac{\sum || F(h0l_{obs}| - |F(h0l)_{calc} ||}{\sum |F(h0l)_{obs}|}$$

as low as 0.20. It was thus thought that this structure proposal should not be very different from the actual structure, which, however, might lack the centre of symmetry.

In order to find the *y* coordinates corresponding to the approximate structure, the [100] projection of the Patterson function was studied (*cf.* Fig. 3 : 1). In this way it was possible to find the metal atom coordinates. However, when calculating the *F(hkl)* values, it was observed that the agreement was rather poor for the weak layer lines with *k* odd.

* During the later stages of the investigation the computational work was highly facilitated by the employment of the electronic digital computer BESK of the Swedish Board of Computing Machinery. Programmes for automatic Patterson and electron density syntheses and for automatic calculation of structure factors have been prepared by members of this research group [14,15].

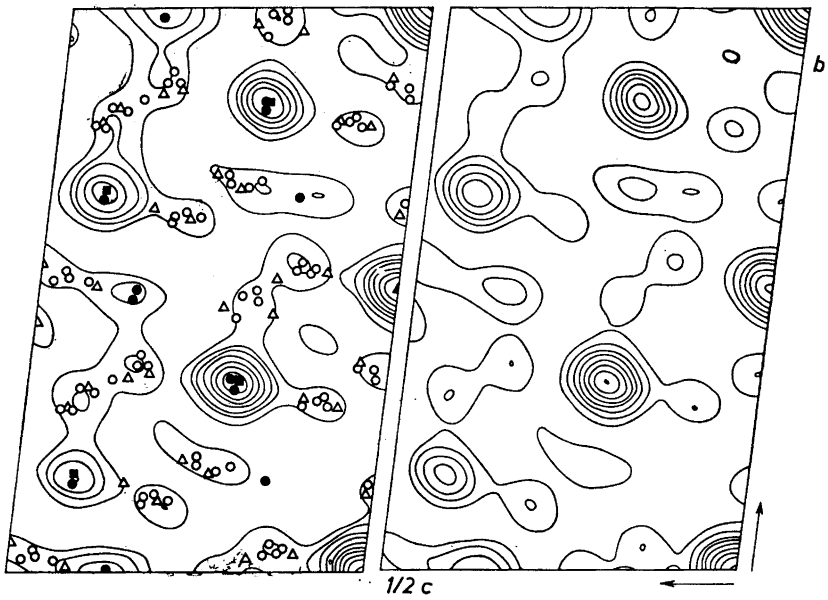

Fig. 3. Patterson projections along [100]. 1) Calculated from $|F|^2_{obs}$. 2) Calculated from $|F|^2_{calc}$. ▲ : Ti-Ti vectors (Multiplicity 10); ■ : Ti-Ti vectors (Multiplicity 4]; ● : Ti-Ti vectors (Multiplicity 2); O: Ti-O vectors (Multiplicity 2); △: Ti-O vectors (Multiplicity 1).

Starting from the approximate centrosymmetric structure thus derived, the metal atom positions were modified to improve the agreement with the Patterson function. The changes of the coordinates were considerable only for one of the ten titanium atoms and implies that the symmetry of the structure was lowered to $P1$. The electron density projections parallel to [010] and [100] calculated on the basis of the modified structure showed maxima interpretable as due to all the titanium and oxygen atoms of the unit cell.

The agreement between the Patterson functions calculated from the observed and the corresponding calculated $|F|^2$ values and the interatomic vector sets required by the structure is demonstrated in Figs. 2 and 3 and Table 1.

In Fig. 3 : 1 it can be seen that there is no maximum in the Patterson projection corresponding to the titanium-titanium vector of the lowest multiplicity required by the structure. Such a phenomenon has been demonstrated by Magnéli [13] to be due to the large number of non-observed reflexions. Thus the Patterson projection calculated from $|F|^2_{calc}$ omitting all reflexions below "the limit of visibility" (Fig. 3 : 2) does not show a maximum corresponding to this titanium-titanium vector. The two weak maxima in Fig. 3 : 1, which are not required by the metal atom structure correspond to the oxygen-oxygen vectors of highest multiplicity.

Table 1. Patterson projections along [010] and [100]. Comparison between observed and calculated coordinates and the heights of the corresponding maxima.

x_{obs} / x_{calc}	z_{obs} / z_{calc}	height$_{obs}$ / height$_{calc}$	y_{obs} / y_{calc}	z_{obs} / z_{calc}	height$_{obs}$ / height$_{calc}$
0.182	0.097	6	0.355	0.004	3
0.178	0.093	9	0.346	0.002	4
0.379	0.124	5	0.500	0.000	29
0.383	0.127	8	0.500	0.000	28
0.657	0.020	9	0.469	0.203	3
0.655	0.015	8	0.482	0.208	3
0.706	0.150	6	0.548	0.140	5
0.713	0.150	6	0.547	0.137	5
0.919	0.196	9	0.665	0.123	4
0.917	0.201	9	0.668	0.130	4
0.571	0.211	37	0.677	0.200	4
0.572	0.215	41	0.676	0.206	5
0.223	0.235	7	0.626	0.302	2
0.220	0.231	5	0.623	0.303	4
0.135	0.421	26	0.789	0.420	5
0.136	0.423	29	0.806	0.425	4
0.294	0.368	16	0.995	0.366	11
0.293	0.365	18	0.997	0.359	12
0.489	0.415	7	0.786	0.080	3
0.485	0.422	8	0.785	0.081	5
0.749	0.314	5	0.834	0.212	21
0.747	0.310	6	0.833	0.212	22
0.786	0.449	6	0.865	0.012	2
0.783	0.446	4	0.852	0.007	3
0.948	0.357	6	0.917	0.094	3
0.950	0.351	8	0.916	0.093	0
0.039	0.133	4	0.980	0.207	4
0.039	0.133	4	0.987	0.214	5
0.187	0.217	2	0.117	0.295	3
0.182	0.216	4	0.115	0.297	5
0.293	0.086	3	0.171	0.422	12
0.291	0.086	4	0.169	0.425	14
0.334	0.213	28	0.305	0.426	4
0.333	0.214	28	0.314	0.429	4

(Table 1 (contd.)

x_{obs} / x_{calc}	z_{obs} / z_{calc}	height$_{obs}$ / height$_{calc}$	x_{obs} / x_{calc}	z_{obs} / z_{cac}	height$_{obs}$ / height$_{calc}$
0.372	0.358	4	0.887	0.363	5
0.366	0.354	4	0.875	0.358	4
0.496	0.377	5	0.550	0.491	2
0.500	0.367	6	0.548	0.485	3
0.672	0.425	18			
0.669	0.427	19			

The index of agreement, R, for the two projections [010] and [100] was found to be 0.13 and 0.15, respectively. For all the 272 registered reflexions, the R-value is 0.18. The 19 observed reflexions hkl with k odd, which are due only to the oxygen atom contributions have $R = 0.10$, which indicates that the oxygen atom positions should be fairly accurate. Table 2 gives the observed and calculated F values for reflexions $h0l$, $0kl$ and hll.

DESCRIPTION OF THE STRUCTURE

The structure is built up of TiO_6 octahedra which are joined by sharing corners, edges and faces. All the interatomic distances are of reasonable lengths, *viz.* 2.81—3.19 Å for the Ti-Ti distances, 1.75—2.35 Å for the Ti-O and 2.4—3.15 Å for the O—O distances. The shortest Ti-Ti distance connects the metal atoms of TiO_6 octahedra with a face in common.

The oxygen atom packing is roughly a deformed hexagonal close packing and similar to that of rutile. The structure may be described as being built up of rutile-type elements, with a complicated arrangement of the metal atoms in the interstitial positions of the lattice formed by the anion packing.

The metal atom positions in the projections along [010] and [100] are shown in Figs. 4 and 5. The dotted lines refer to an alternative origin, which apparently is a centre of symmetry for the metal atom arrangement. However, this is not true since it has a significant deviation from centrosymmetry. The origin chosen was preferred because it emphasizes the true centrosymmetry found to be present in the arrangement of the oxygen atoms.

In both projections the metal atoms form chains of five TiO_6-octahedra (if these chains were of infinite length, the structure would be rutile). The chains are connected to form rutile-type slabs possessing an infinite extension in two dimensions and a characteristic finite width (five TiO_6-octahedra) *i.e.* the length of the chain in a third direction, indicated by arrows in Fig. 5. The mutual connection of the slabs takes place by means of TiO_6-octahedra sharing faces.

Table 2. Observed and calculated structure factors *h0l*, *0kl* and *h1l* for Ti_5O_9. The values of the phase angle, α are expressed as fractions of one cycle.

h 0 l	$\|F\|_{obs}$	$\|F\|_{calc}$	α	*h 0 l*	$\|F\|_{abs}$	$\|F\|_{calc}$	α
2 0 $\bar{11}$	<18	4	0.427	4 0 $\bar{3}$	<35	19	0.366
3 0 $\bar{11}$	<20	8	0.389	5 0 $\bar{3}$	<38	4	0.748
4 0 $\bar{11}$	65	59	0.969	6 0 $\bar{3}$	<30	22	0.969
0 0 $\bar{10}$	56	45	0.947	0 0 $\bar{2}$	26	14	0.742
1 0 $\bar{10}$	<25	13	0.176	1 0 $\bar{2}$	62	72	0.064
2 0 $\bar{10}$	77	82	0.510	2 0 $\bar{2}$	52	38	0.851
3 0 $\bar{10}$	<30	7	0.566	3 0 $\bar{2}$	25	31	0.153
4 0 $\bar{10}$	<27	14	0.128	4 0 $\bar{2}$	<35	22	0.859
5 0 $\bar{10}$	<22	27	0.911	5 0 $\bar{2}$	<37	17	0.078
0 0 $\bar{9}$	67	74	0.037	6 0 $\bar{2}$	111	105	0.498
1 0 $\bar{9}$	<34	18	0.839	0 0 $\bar{1}$	13	11	0.374
2 0 $\bar{9}$	<36	18	0.086	0 0 $\bar{1}$	13	11	0.374
3 0 $\bar{9}$	<36	5	0.518	1 0 $\bar{1}$	25	27	0.683
4 0 $\bar{9}$	<35	13	0.895	2 0 $\bar{1}$	110	104	0.455
5 0 $\bar{9}$	80	81	0.473	3 0 $\bar{1}$	31	27	0.697
6 0 $\bar{9}$	<17	17	0.682	4 0 $\bar{1}$	48	52	0.061
0 0 $\bar{8}$	<36	25	0.641	5 0 $\bar{1}$	<36	17	0.888
1 0 $\bar{8}$	60	43	0.429	6 0 $\bar{1}$	<23	10	0.468
2 0 $\bar{8}$	<38	21	0.606	0 0 0	–	364	0.000
3 0 $\bar{8}$	101	117	0.006	1 0 0	22	18	0.259
4 0 $\bar{8}$	<35	10	0.081	2 0 0	60	50	0.581
5 0 $\bar{8}$	49	51	0.538	3 0 0	55	38	0.391
6 0 $\bar{8}$	36	33	0.425	4 0 0	<38	20	0.734
0 0 $\bar{7}$	<38	20	0.228	5 0 0	<34	24	0.408
1 0 $\bar{7}$	<37	34	0.608	6 0 0	<17	6	0.649
2 0 $\bar{7}$	<36	20	0.340	1 0 1	34	21	0.079
3 0 $\bar{7}$	<37	9	0.777	2 0 1	<26	19	0.725
4 0 $\bar{7}$	<38	10	0.979	3 0 1	85	92	0.038
5 0 $\bar{7}$	<36	10	0.256	4 0 1	<38	20	0.760
6 0 $\bar{7}$	58	66	0.965	5 0 1	78	90	0.474
0 0 $\bar{6}$	<35	27	0.866	1 0 2	97	103	0.505
1 0 $\bar{6}$	33	25	0.196	2 0 2	<29	14	0.229
2 0 $\bar{6}$	62	53	0.936	3 0 2	59	59	0.948
3 0 $\bar{6}$	<36	14	0.173	4 0 2	44	33	0.099
4 0 $\bar{6}$	80	94	0.505	5 0 2	<26	17	0.827
5 0 $\bar{6}$	<37	16	0.568	1 0 3	<26	4	0.619
6 0 $\bar{6}$	<28	23	0.094	2 0 3	<32	21	0.567
0 0 $\bar{5}$	116	113	0.472	3 0 3	<37	18	0.325
1 0 $\bar{5}$	32	26	0.741	4 0 3	70	72	0.540
2 0 $\bar{5}$	114	133	0.029	1 0 4	<31	7	0.313
3 0 $\bar{5}$	30	33	0.914	2 0 4	80	82	0.008
4 0 $\bar{5}$	<36	8	0.157	3 0 4	<36	12	0.772
5 0 $\bar{5}$	<38	10	0.447	4 0 4	54	45	0.444
6 0 $\bar{5}$	<30	13	0.853	1 0 5	<35	12	0.657
0 0 $\bar{4}$	38	35	0.589	2 0 5	<38	5	0.000
1 0 $\bar{4}$	42	39	0.375	3 0 5	<33	15	0.097
2 0 $\bar{4}$	25	34	0.651	4 0 5	<16	13	0.779
3 0 $\bar{4}$	58	55	0.438	1 0 6	<38	25	0.087
4 0 $\bar{4}$	<35	17	0.613	2 0 6	<36	4	0.729
5 0 $\bar{4}$	87	83	0.001	3 0 6	96	112	0.507
6 0 $\bar{4}$	<30	11	0.125	1 0 7	87	89	0.974
0 0 $\bar{3}$	24	17	0.217	2 0 7	<30	7	0.187
1 0 $\bar{3}$	105	142	0.968	1 0 8	<30	20	0.361
2 0 $\bar{3}$	32	33	0.180	2 0 8	<18	15	0.599
3 0 $\bar{3}$	116	139	0.527	1 0 9	<20	16	0.691

Table 2 (cont.)

0 *k l*	$\lvert F\rvert_{obs}$	$\lvert F\rvert_{calc}$	α	0 *k l*	$\lvert F\rvert_{obs}$	$\lvert F\rvert_{calc}$	α
0 0 $\bar{10}$	56	45	0.946	0 0 $\bar{5}$	24	17	0.278
0 1 $\bar{10}$	<22	4	0.997	0 1 $\bar{3}$	<22	8	0.000
0 2 $\bar{10}$	<23	13	0.212	0 2 $\bar{3}$	81	97	0.021
0 3 $\bar{10}$	<23	3	0.006	0 3 $\bar{3}$	<26	3	0.478
0 4 10	28	16	0.016	0 4 $\bar{3}$	<30	26	0.804
0 5 $\bar{10}$	<16	3	0.483	0 5 $\bar{3}$	<35	3	0.967
0 0 $\bar{9}$	67	74	0.038	0 6 $\bar{3}$	<38	14	0.212
0 1 $\bar{9}$	<31	10	0.002	0 7 $\bar{3}$	<36	1	0.478
0 2 $\bar{9}$	<32	12	0.733	0 8 $\bar{3}$	103	91	0.008
0 3 $\bar{9}$	26	29	0.000	0 0 $\bar{2}$	26	14	0.749
0 4 $\bar{9}$	<30	5	0.765	0 1 $\bar{2}$	<17	2	0.498
0 5 $\bar{9}$	<27	8	0.508	0 2 $\bar{2}$	49	35	0.594
0 6 $\bar{9}$	59	73	0.034	0 3 $\bar{2}$	<25	7	0.511
0 0 $\bar{8}$	<36	25	0.657	0 4 $\bar{2}$	88	100	0.459
0 1 $\bar{8}$	<38	2	0.510	0 5 $\bar{2}$	<35	4	0.475
0 2 $\bar{8}$	82	97	0.484	0 6 $\bar{2}$	<38	16	0.621
0 3 $\bar{8}$	<37	3	0.500	0 7 $\bar{2}$	<36	1	0.994
0 4 $\bar{8}$	<35	11	0.362	0 8 $\bar{2}$	37	32	0.537
0 5 $\bar{8}$	<33	5	0.015	0 0 $\bar{1}$	13	11	0.375
0 6 $\bar{8}$	<28	27	0.609	0 1 $\bar{1}$	<15	3	0.504
0 7 $\bar{8}$	<19	1	0.571	0 2 $\bar{1}$	34	28	0.179
0 0 $\bar{7}$	<38	20	0.203	0 3 $\bar{1}$	<24	6	0.014
0 1 $\bar{7}$	<38	1	0.489	0 4 $\bar{1}$	47	62	0.565
0 2 $\bar{7}$	<38	7	0.685	0 5 $\bar{1}$	<35	5	0.983
0 3 $\bar{7}$	<38	5	0.002	0 6 $\bar{1}$	<38	17	0.067
0 4 $\bar{7}$	51	38	0.947	0 7 $\bar{1}$	<35	2	0.509
0 5 $\bar{7}$	<37	1	0.921	0 8 $\bar{1}$	<24	19	0.088
0 6 $\bar{7}$	<33	25	0.129	0 0 0	—	364	0.000
0 7 $\bar{7}$	<26	5	0.478	0 1 0	<14	1	0.511
0 0 $\bar{6}$	<35	27	0.839	0 2 0	42	33	0.170
0 1 $\bar{6}$	<34	2	0.507	0 3 0	85	80	0.001
0 2 $\bar{6}$	<34	8	0.439	0 4 0	18	28	0.850
0 3 $\bar{6}$	<35	2	0.986	0 5 0	<36	2	0.969
0 4 $\bar{6}$	46	60	0.043	0 6 0	113	117	0.004
0 5 $\bar{6}$	<38	5	0.479	0 7 0	<34	2	0.980
0 6 $\bar{6}$	<36	19	0.780	0 8 0	<21	12	0.263
0 7 $\bar{6}$	<30	28	0.503	0 1 1	<16	0	0.134
0 8 $\bar{6}$	<19	10	0.425	0 2 1	86	77	0.564
0 0 $\bar{5}$	116	113	0.470	0 3 1	<26	1	0.590
0 1 $\bar{5}$	<30	3	0.496	0 4 1	<32	20	0.238
0 2 $\bar{5}$	<30	1	0.158	0 5 1	<37	10	0.005
0 3 $\bar{5}$	<32	2	0.025	0 6 1	<38	16	0.495
0 4 $\bar{5}$	34	31	0.607	0 7 1	<31	6	0.011
0 5 $\bar{5}$	<38	6	0.084	0 1 2	<20	4	0.994
0 6 $\bar{5}$	82	93	0.470	0 2 2	87	90	0.448
0 7 $\bar{5}$	<33	4	0.020	0 3 2	<29	1	0.428
0 8 $\bar{5}$	<24	3	0.901	0 4 2	<34	16	0.720
0 0 $\bar{4}$	38	35	0.575	0 5 2	<38	9	0.997
0 1 $\bar{4}$	<25	2	0.503	0 6 2	<36	5	0.863
2 0 $\bar{4}$	33	18	0.943	0 7 2	<27	1	0.614
0 3 $\bar{4}$	<29	0	0.621	0 1 3	81	82	0.500
0 4 $\bar{4}$	23	23	0.206	0 2 3	41	44	0.898
0 5 $\bar{4}$	<36	3	0.462	0 3 3	<32	10	0.506
0 6 $\bar{4}$	<38	23	0.626	0 4 3	64	58	0.033
0 7 $\bar{4}$	<35	4	0.513	0 5 3	<38	7	0.001
0 8 $\bar{4}$	37	24	0.992	0 6 3	<33	9	0.366

Table 2 (cont.)

0 k l	$\|F\|_{obs}$	$\|F\|_{calc}$	a	0 k l	$\|F\|_{obs}$	$\|F\|_{calc}$	a
0 7 3	<20	23	0.496	0 2 6	104	108	0.026
0 1 4	<28	1	0.981	0 3 6	<37	8	0.496
0 2 4	<31	24	0.246	0 4 6	<32	5	0.986
0 3 4	<36	7	0.493	0 5 6	<22	23	0.002
0 4 4	<38	9	0.832	0 1 7	<38	1	0.466
0 5 4	<36	3	0.497	0 2 7	<36	26	0.918
0 6 4	43	41	0.537	0 3 7	<32	1	0.529
0 1 5	<33	1	0.039	0 4 7	<23	10	0.544
0 2 5	<35	28	0.633	0 1 8	<34	3	0.506
0 3 5	<38	6	0.507	0 2 8	<29	13	0.351
0 4 5	<37	4	0.312	0 3 8	<22	4	0.002
0 5 5	<30	4	0.506	0 1 9	<25	1	0.488
0 6 5	61	72	0.476	0 2 9	<17	7	0.752
0 1 6	<37	2	0.991				

In the rutile structure there are channels of empty interstitial positions along the *c* axis ($\frac{1}{2}00$ or $\frac{1}{2}0\frac{1}{2}$). In the Ti_5O_9 structure the end atoms of the chains (*cf.* Figs. 4 and 5) occupy such positions of the neighbouring rutile slabs. The latter are thus mutually "out of phase" by $\frac{1}{2}(b_r + c_r)$ (*cf.* Fig. 6), which gives rise to a so called" shear structure". A term introduced by Wadsley [17].

The structure of the shear plane (the border region of the two "out of phase" rutile-type blocks) is closely related to the corundum-structure type. Thus, parallel to the *b* axis of Ti_5O_9, infinite chains of double-octahedra are found, the doublets being formed by two single TiO_6-octahedra sharing a face. The double octahedra are coupled together within the chains by having edges in common (*cf.* Fig. 7 : 1). These chains are included in the rutile-typs slabs, the connection taking place by octahedra sharing edges and corners (Fig. 7 : 2).

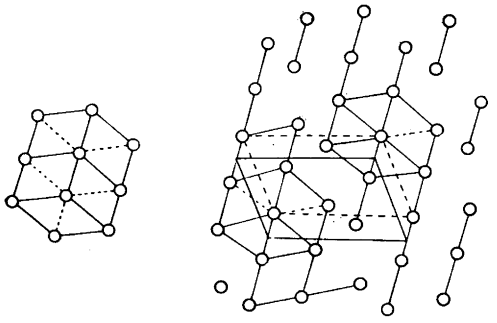

Fig. 4. The metal atom arrangement of Ti_5O_9 viewed along [010] and of rutile parallel to [111].

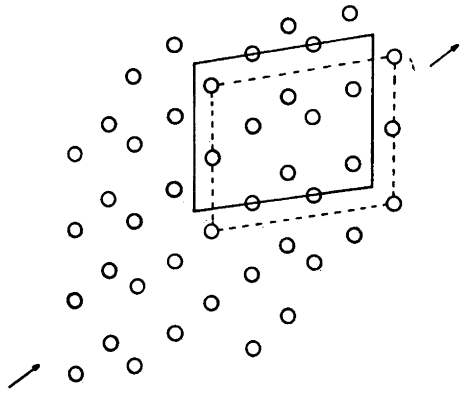

Fig. 5. The metal atom arrangement of Ti_5O_9 viewed along [100]. The arrows show the direction of the finite extension of the rutile slabs.

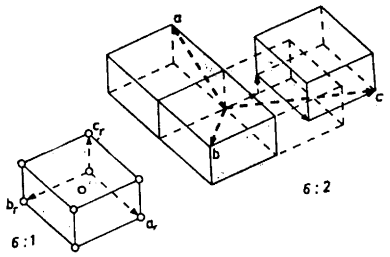

Fig. 6. 1) Unit cell of rutile with positions of metal atoms indicated. 2) Interrelation of basic rutile-type structure of adjacent slabs of Ti_5O_9. Unit cell axes of the latter indicated by dashed heavily-drawn arrows.

The metal-metal distance over the common face is 2.81 Å, while the distance between metal atoms over the common edge is 3.19 Å. The corresponding distance [16] for Ti_2O_3 are 2.56 and 2.99 Å.

The shearing mechanism can be described by means of a translation matrix. Fig. 6 demonstrates the interrelation of the basic rutile-type structure of adjacent slabs of Ti_5O_9. If the axes of the rutile-type subunit cell $\boldsymbol{a}_r$, $\boldsymbol{b}_r$ and $\boldsymbol{c}_r$ are used to define the coordinate system, then the axes of the ideal Ti_5O_9 unit cell will be:

$$\begin{aligned} \boldsymbol{a} &= \boldsymbol{c}_r - \boldsymbol{a}_r \\ \boldsymbol{b} &= \boldsymbol{a}_r + \boldsymbol{b}_r + \boldsymbol{c}_r \\ \boldsymbol{c} &= \boldsymbol{a}_r - \tfrac{3}{2}\,\boldsymbol{b}_r - \tfrac{1}{2}\,\boldsymbol{c}_r \end{aligned}$$

The matrix

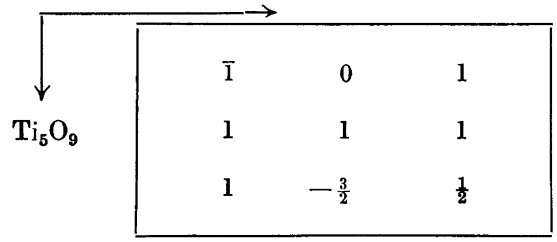

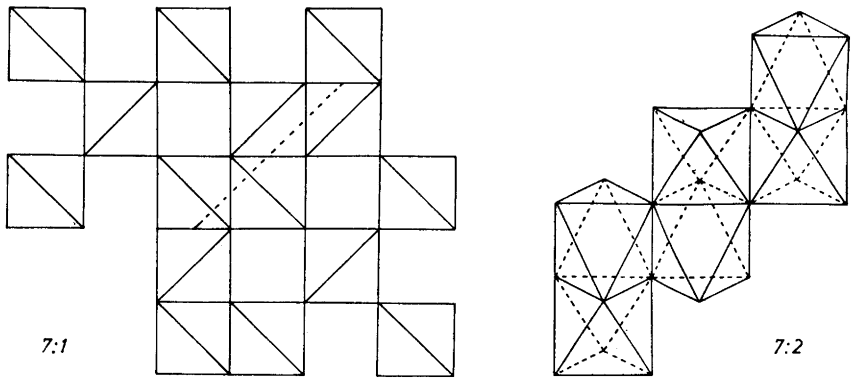

Fig. 7. 1) Projection of part of the Ti_5O_9 structure along the subcell c-axis showing the shear mechanism. The dotted line is parallel to the b-axis and the shear chain of the corundum structure. 2) The shear chain of the corundum structure.

thus makes it possible to obtain the relation between the indices of Ti_5O_9 and rutile.

If the vectorial equations given above are solved for a_r, b_r and c_r, the following expressions are obtained:

$$a_r = \tfrac{1}{9}(-4a + 3b + 2c)$$
$$b_r = \tfrac{1}{9}(-a + 3b - 4c)$$
$$c_r = \tfrac{1}{9}(5a + 3b + 2c)$$

The matrix

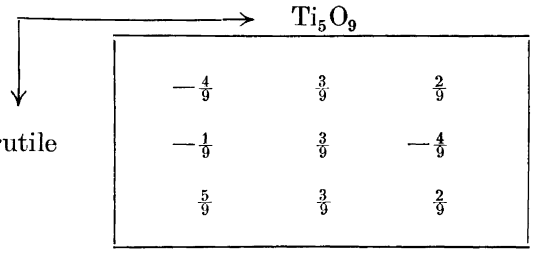

thus interrelates the atomic positions x, y, and z of Ti_5O_9 with those in the coordinate system difined by the rutile-type subcell ($x_r y_r$ and z_r).

By means of the latter matrix it has thus been possible to calculate the "ideal" atomic positions of the structure of Ti_5O_9 (Table 3). The deviation for some atoms from the coordinates of the actual structure should be due to the repulsion between the close metal atoms of octahedra sharing faces.

DISCUSSION OF THE STRUCTURE

It is of considerable interest to compare the structures of Ti_5O_9 and the homologues Ti_nO_{2n-1} with the structures previously found by Magnéli [6] for the series M_nO_{3n-1} and M_nO_{3n-2}. There are, of course, no obvious geometrical rela-

Table 3. Comparison between observed and ideal atomic coordinates for Ti_5O_9.

Atom	Observed coordinates			Ideal coordinates			Atom	Observed coordinates			Ideal coordinates		
	x	y	z	x	y	z		x	y	z	x	y	z
Ti_1	0.276	0.170	0.107	0.278	0.167	0.111	O_5	0.67	0.70	0.23	0.66	0.70	0.27
Ti_2	0.276	0.670	0.107	0.278	0.667	0.111	O_6	0.20	0.65	0.30	0.18	0.67	0.32
Ti_3	0.852	0.008	0.316	0.833	0.000	0.333	O_7	0.51	0.37	0.36	0.49	0.33	0.35
Ti_4	0.852	0.502	0.316	0.833	0.500	0.333	O_8	0.99	0.30	0.43	0.00	0.30	0.40
Ti_5	0.575	0.170	0.470	0.611	0.167	0.444	O_9	0.24	0.04	0.46	0.22	0.04	0.49
Ti_6	0.575	0.670	0.470	0.611	0.667	0.444	O_{10}	0.76	0.96	0.54	0.78	0.96	0.51
Ti_7	0.148	0.992	0.684	0.167	0.000	0.667	O_{11}	0.01	0.70	0.57	0.00	0.70	0.60
Ti_8	0.148	0.492	0.684	0.167	0.500	0.667	O_{12}	0.49	0.63	0.64	0.51	0.67	0.65
Ti_9	0.724	0.330	0.893	0.722	0.333	0.889	O_{13}	0.80	0.35	0.70	0.82	0.33	0.69
Ti_{10}	0.724	0.830	0.893	0.722	0.833	0.889	O_{14}	0.33	0.30	0.77	0.34	0.30	0.74
							O_{15}	0.53	0.03	0.80	0.55	0.04	0.82
O_1	0.63	0.32	0.11	0.62	0.33	0.09	O_{16}	0.08	0.99	0.88	0.07	0.00	0.87
O_2	0.11	0.38	0.03	0.11	0.37	0.04	O_{17}	0.89	0.62	0.97	0.89	0.63	0.96
O_3	0.92	0.01	0.12	0.94	0.00	0.13	O_{18}	0.37	0.68	0.89	0.38	0.67	0.91
O_4	0.47	0.97	0.20	0.45	0.96	0.18							

tions, because the subcells of rutile and of ReO_3-type are quite different. However, the principles for deriving the geometrical relations in each series are exactly the same. For example, in Mo_8O_{23} the major structural elements of the ReO_3-type structure are characterized by a finite width of 8 MoO_6 octahedra. In Mo_9O_{26}, the width of the slabs is extended to comprise one more MoO_6 octahedron. In any member of the series M_nO_{3n-1} there are two constant axes, a and b, parallel to the shear plane, while the c axis is determined by the thickness of the ReO_3-blocks and thus increases with n.

In the series Ti_nO_{2n-1}, V_nO_{2n-1} and $Ti_{n-2}Cr_2O_{2n-1}$ the same characteristics have been observed. The a and b axes and the angle γ all remain constant irrespective of the value of n, while the length and direction of the c axis are determined by the finite width of the rutile-type slabs and are thus functions of n. General structural data for the three series M_nO_{2n-1} have been derived from the matrices given above and will be reported elsewhere.

Acknowledgements. The author wishes to express his sincere gratitude to Professor A. Ölander for his kind interest and to the principal investigator of this research programme, Dr. Arne Magnéli, for having suggested this investigation, for his never-failing interest and for many valuable discussions. I also want to thank Miss Lena Jahnberg for her valuable assistance in the calculations.

The investigation has been sponsored in part by the *Office, Chief of Research and Development, U.S. Department of Army,* through its European Research Office and in part by the *Swedish Natural Science Research Council.*

REFERENCES

1. Andersson, S. and Magnéli, A. *Naturwiss.* **43** (1956) 495.
2. Andersson, S., Collén, B., Kuylenstierna, U. and Magnéli, A. *Acta Chem. Scand.* **11** (1957) 1641.
3. Andersson, S. *XVI^e Congrès International de Chimie Pure et Appliquée,* Paris 1957. Memoires présentés à la Section de Chimie Minérale 53.
4. Andersson, S., Sundholm, A. and Magnéli, A. *Acta Chem. Scand.* **13** (1959) 989.
5. Andersson, G. *Acta Chem. Scand.* **8** (1954) 1599.
6. Magnéli, A. *Acta Cryst.* **6** (1953) 495.
7. Blomberg, B., Kihlborg, L. and Magnéli, A. *Arkiv Kemi* **6** (1953) 133.
8. Magnéli, A., Blomberg-Hansson, B., Kihlborg, L. and Sundkvist, G. *Acta Chem. Scand.* **9** (1955) 1382.
9. Andersson, S. and Jahnberg, L. *To be published.*
10. Westman, S. and Magnéli, A. *Acta Chem. Scand.* **11** (1957) 1587.
11. Andersson, S., Collén, B., Kruuse, G., Kuylenstierna, U., Magnéli, A., Pestmalis, H. and Åsbrink, S. *Acta Chem. Scand.* **11** (1957) 165.
12. Magnéli, A. *Arkiv Kemi* **1** (1950) 513.
13. Magnéli, A. *Acta Cryst.* **4** (1951) 447.
14. Westman, S., Blomqvist, G. and Åsbrink, S. *Arkiv Kemi* **14** (1959) 535.
15. Åsbrink, S., Blomqvist, G. and Westman, S. *Arkiv Kemi* **14** (1959) 545.
16. Nordmark, Claes. *To be published.*
17. Wadsley, A. D. *Revs. Pure Appl. Chem.* **5** (1955) 165.

Received February 19, 1960.